Atomistic Determination of Continuum Mechanical Properties of Ion-Bombarded Silicon

N. Kalyanasundaram
Department of Mechanical and Industrial Engineering,
University of Illinois at Urbana-Champaign

J. B. Freund
Department of Theoretical and Applied Mechanics,
University of Illinois at Urbana-Champaign

H. T. Johnson
Department of Mechanical and Industrial Engineering,
University of Illinois at Urbana-Champaign

Highly disordered, ion-processed silicon is studied using a molecular dynamics simulation with empirical interatomic potentials. The surface free energy density, stress-strain relations, and continuum surface features of silicon, bombarded in the simulations to relatively high fluence by medium energy argon ions, are computed statistically by preparing multiple randomized ion-bombarded specimens. The surface-free energy per unit area for the ion-bombarded silicon is about $1.76\ \mathrm{J/m^2}$*, much lower than the* $2.35\ \mathrm{J/m^2}$ *corresponding to a (001) unrelaxed, crystalline silicon surface. A stress-strain curve is obtained computationally by performing a constant strain test on the ion-bombarded specimens and by calculating stresses from the interatomic forces acting across different cross sections in the sample. The resulting tensile elastic modulus of the material, while slightly elevated due to the prominence of the free surface in the thin layer, is in good agreement with available experimental data. The surface is characterized using an interatomic potential-based* C^2 *continuous sampling method.* [DOI: 10.1115/1.2020014]

1 Introduction

Ion bombardment is one of the most important processing methods in electronic materials. It has been widely used for many years for mild surface modification as well as for ion-implantation doping. More recently it has been used for other purposes in nano- and microscale electronic materials applications, including for intentional tailoring of stress in Microelectromechanical Systems (MEMS) devices [1]. It has also been shown to create surface nanostructures in semiconducting materials [2,3]. Similar formation of nanostructures such as quantum dots has been demonstrated during the epitaxial growth of Ge on Si [4–6]. It is now well known that the electronic and optical properties of these nanostructures depend on the shape, size, and number density [7]. Furthermore, fundamental mechanical properties such as surface free energy per unit area and constitutive relations of the material near the surface play an important role in the evolution of surfaces and in the development of the characteristics that govern the device properties. Use of ion bombardment to fabricate silicon nanostructures alters the property of target material (initially crystalline silicon) at and near the surface due to implantation, sputtering, and transformation from crystalline to amorphous phase [8]. In order to understand the evolution of nanostructures due to ion bombardment, it is critical, then, to determine the surface-free energies and constitutive behavior of the ion bombarded target material and to characterize the atomistic surface from a convenient continuum perspective. In this work, argon ion bombarded silicon samples are prepared using molecular dynamics (MD). Empirical interatomic potentials are used to calculate surface free energy per unit area, stress-strain relations, and a useful continuum mapping for the disordered atomistic surfaces under consideration.

The shape and size evolution of nanostructures can be determined by obtaining the near-surface geometric configuration that minimizes the total free energy, where the total free energy is usually the sum of energy required to create a surface and the strain energy associated with forming the surface. The Stranski-Krastanow growth process by which islands form due to lattice mismatch in an epitaxial growth process is often described in terms of this minimization of total free energy, cast in terms of gradients of chemical potential [9]. Knowledge of absolute surface free energy, constitutive relations, diffusion coefficient, initial conditions, and perturbations is needed to compute surface evolution in this manner. These quantities, in particular surface free energy and surface diffusion coefficient, are difficult to measure experimentally. Computational methods to calculate free energy and constitutive relations typically employ either an empirical interatomic potential or use tight-binding methods to predict atomic or molecular trajectories. A statistical description of observables is then extracted from the simulation results.

2 Simulation Methodology

The focus of the present work is on single-crystal silicon. The sample is modeled by a periodically replicated cubic unit cell with side length 5.43 nm which is bombarded with 500 eV argon ions. The ions are incident at randomly selected positions on the (001) surface of the target material. Figure 1 shows a schematic of the simulation. As the fluence (incident ion count per unit surface area) increases, damage propagates into the specimen as the atoms at and near the surface rearrange or sputter, or as the incident argon atoms implant in the specimen. The beam energy considered here is in the same range as that used in nanostructure fabrication. The ion bombardment process is simulated until a steady state, in terms of both structural features and sputtering behavior, is obtained. At steady state, two regions separated by a relatively flat interface are evident in the specimen, as shown in Fig. 1. The upper layer is a predominantly damaged, nearly amorphous layer made of silicon and argon atoms, while the bottom layer is essentially undamaged, argon-free crystalline silicon [8].

Classical molecular dynamics methods are used. The equations of motion are integrated using the velocity-Verlet algorithm to obtain the trajectories. The widely used Stillinger-Weber potential [10] models silicon-silicon interactions. Argon-silicon and argon-argon interactions are modeled by a Moliére potential [11,12] given by

Contributed by the Materials Division of ASME for publication in the Journal of Engineering Materials and Technology. Manuscript received by the Materials Division February 4, 2005; revision received July 12, 2005. Review conducted by: K. Gall.

Copyright © 2005 by ASME

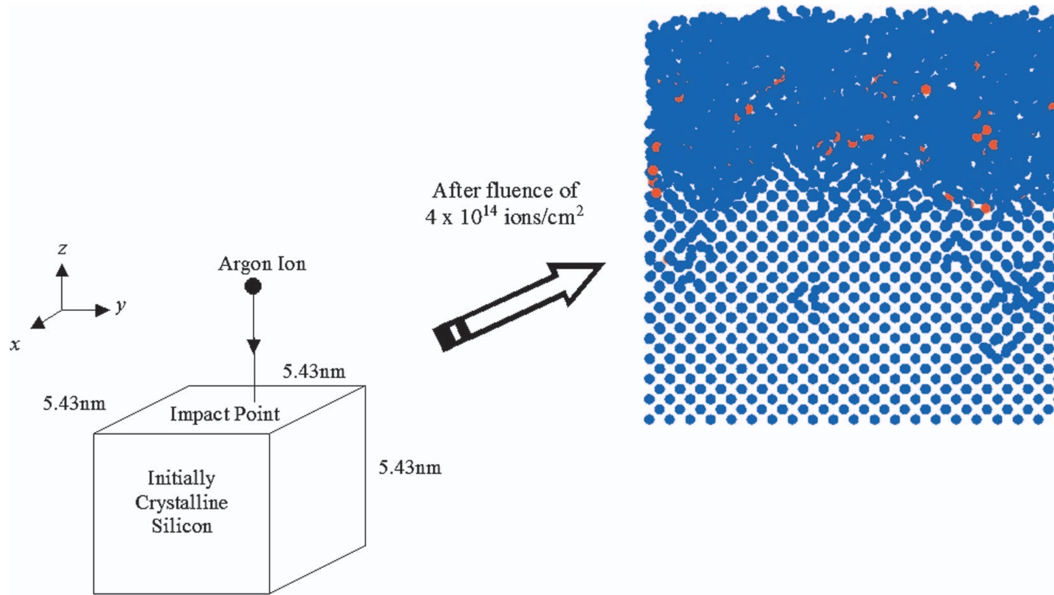

Fig. 1 Schematic of the configuration used to create an ion-bombarded specimen. Molecular dynamics is used to obtain the structure. An argon ion beam at 500 eV beam energy is incident on the [001] surface of initially crystalline silicon. The damage induced after a fluence of 3.39×10^{14} ions/cm^2, as seen in a plane parallel to the $y-z$ axis is shown on the right. The red circles are argon atoms and the blue circles are silicon atoms.

$$\Phi = Z_i Z_j \frac{q^2}{r}\left\{0.35\exp\left(-0.3\frac{r}{a}\right) + 0.55\exp\left(-1.2\frac{r}{a}\right) + 0.10\exp\left(-6.0\frac{r}{a}\right)\right\}, \quad (1)$$

where, Z_i and Z_j are the atomic numbers of either argon or silicon, q is the fundamental unit charge, r is the distance between atoms, and a is a screening distance.

For beam energies of 500 eV a steady state, indicated by a nearly steady sputtering and implantation rates and a nearly steady induced compressive stress due to bombardment, is obtained at about a fluence of about 3.39×10^{14} ions/cm^2. The depth of damage from the surface is about 2.2 nm. This fluence may be obtained after only a few seconds of clock time in typical experimental flux conditions, but it represents a substantial computational challenge for studies based on molecular dynamics. The present work captures these long time scales by assuming a low background temperature of 77 K, which suppresses annealing between ion impacts. This allows for the assumption of long elapsed time between ion impacts [8]. This also implies that the simulated beam flux (incident ion count per unit surface area per unit time), or less than 10^{20} ions/cm$^2\cdot$s is well within the range of typical experimental studies. Surface energy, constitutive relations, and a continuum surface definition for a specimen so prepared are calculated using the empirical Stillinger-Weber and Moliére interatomic potentials.

3 Results and Discussion

3.1 Surface Energy. Surface energy of a specimen is dependent on several conditions including surface reconstruction, other structural relaxation, and near-surface temperature. Controlling these conditions during an experiment is difficult. For this reason, in spite of the importance of this quantity, there are few experimental surface energy data.

In order to measure the surface-free energy computationally, the ion-bombarded sample is first cleaved at a specific depth, parallel to the [001] plane, to create two surfaces separated by vacuum. The specimen average temperature is maintained at 77 K. Treating the static crack that is created as a system in equilibrium and applying the Griffith criterion, the change in energy due to the cleavage is the energy required to create two surfaces [13]. That is,

$$E_{\text{surf}} = \frac{1}{2}\Delta E, \quad (2)$$

where, E_{surf} is the surface energy and ΔE is the change in energy due to creation of two surfaces.

If there are any reconstructions at the surface, the surface energy $E_{\text{surf}}^{n\times m}$, is given by

$$E_{\text{surf}}^{n\times m} = \frac{1}{2}\frac{1}{nm}\left\{E_{\text{tot}} - \frac{nm}{N_{\text{bulk}}}E_{\text{bulk}}\right\}, \quad (3)$$

where, n and m denote an $n\times m$ reconstruction, E_{tot} is the total energy of a small slab containing nm atoms, and E_{bulk} is the reference bulk energy of a cell containing N_{bulk} atoms [14,15]. The creation of two equivalent surfaces is accounted for by dividing the expression by two. The surface energy per unit area is

$$\gamma = \frac{E_{\text{surf}}^{n\times m}}{A}, \quad (4)$$

where, A is the area of an $n\times m$ cell [14].

Though it is possible to define reconstruction for a crystalline material, there is no counterpart for an amorphous material, except for the 1×1 unit cell. In order to compare surface energies for crystalline and amorphous material, only 1×1 unit cells are considered in this work. The conditions maintained in the present analysis permit no reconstruction for crystalline silicon: The specimen is thermostated at 77 K, a temperature at which thermally activated processes are restricted [16], in order to freeze the structure.

The specimen is analyzed at multiple depths along the [001] direction, starting at a height close to the initial surface. A statistical description of surface-free energy per unit area is obtained both by performing calculations on multiple 1×1 unit cells and averaging over multiple, completely randomized ion-bombarded specimens. Figure 2 shows the plot of variation of free energy per

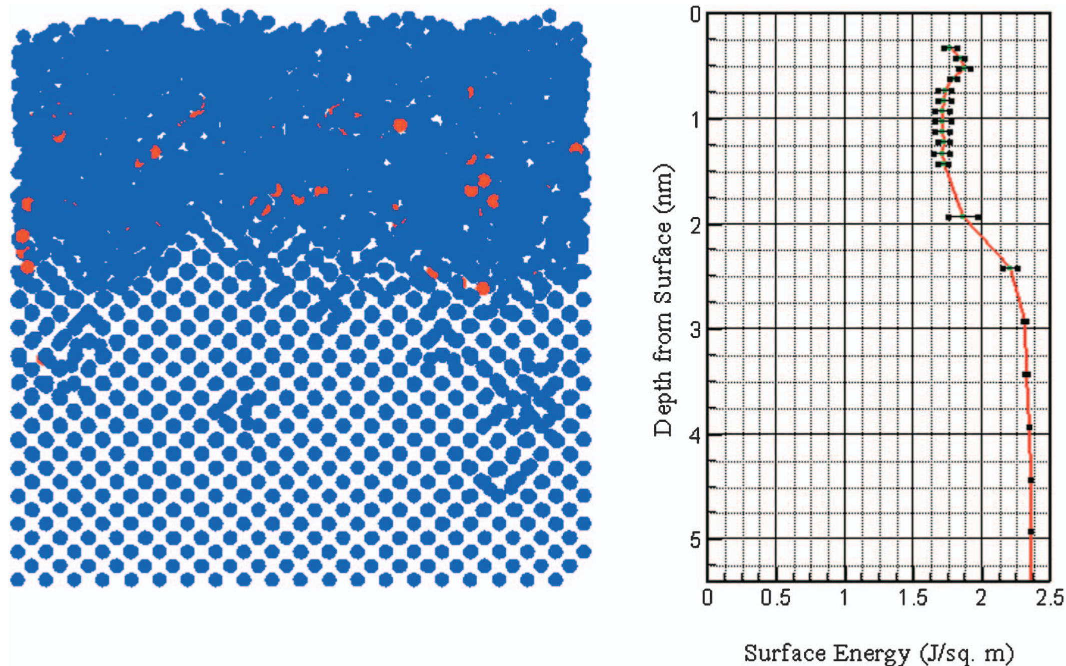

Fig. 2 Variation of surface energy through the depth of the material is shown (right). The figure on the left shows the structure, with the red and blue circles denoting argon and silicon atoms, respectively, seen from a direction parallel to the *y–z* plane, after a steady implantation and sputtering rates are attained. The top, ion damaged portion of the material extends to a depth of about 2.2 nm from the surface. The transition from amorphous, predominantly damaged state to the almost crystalline state is clearly seen in the surface energy graph.

unit area parallel to the surface as a function of depth. In regions where the material is predominantly damaged, the free energy per unit area is determined to be $1.76+/-0.051\ \mathrm{J/m^2}$. The free energy per unit area, corresponding to the (001) surface, for the predominantly defect free, crystalline material is $2.35+/-0.002\ \mathrm{J/m^2}$. The values corresponding to the crystalline material match well with values for unrelaxed crystalline silicon calculated in [14] and in other studies.

The free energy for the ion-bombarded region, which forms the actual surface in an ion-bombarded solid, is lower than that of crystalline silicon by almost 25%. This reduction in surface energy is very nearly in proportion to the reduced average coordination of the atoms in the amorphous region compared to the atoms in the crystalline region. This is to be expected, as fewer bonds must be broken per unit area of new free surface in the amorphous region than in the crystalline region. It is noted that this effect is quite separate from any tendency of a crystalline material to have higher energy density at a free surface due to reduced coordination and corresponding bond reconstructions. Here, the effect is present even several atomic spacings below the surface; the reduced surface energy in the amorphous material relative to the crystalline material is very simply due to a reduced bond density. Such a significantly lower value of surface free energy also implies that in cases where the surface evolution is governed by the Stranski-Krastanow growth mode, even assuming that diffusive mass transport is permitted along the disordered surface, the surface smoothing effect would be much lower in the ion-bombarded material than in crystalline silicon.

3.2 Stress-Strain Relationship. The strain energy stored in the near-surface material because of change in morphology plays an important role in the evolution of nanostructures. An increase in strain energy density stored in the material directly affects the chemical potential and hence the morphology of nanostructures and the rates at which they evolve. The stress strain or constitutive relationship for a material permits computation of strain energy density for a specified value of stress or strain.

Here the ion-bombarded silicon specimen at steady state is subjected to a constant strain test in order to determine some important stress-strain characteristics. Figure 3 shows a schematic of the constant strain test employed in this work. Stresses are calculated in the specimen using a force-balance approach proposed by

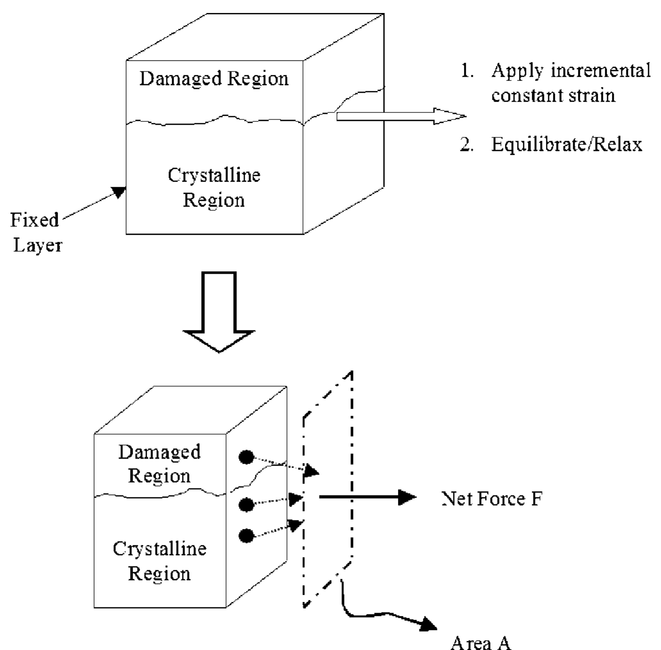

Fig. 3 Schematic illustrating the simulated constant strain test performed to obtain the stress-strain relationship. A force balance approach is used to calculate the mechanical stress.

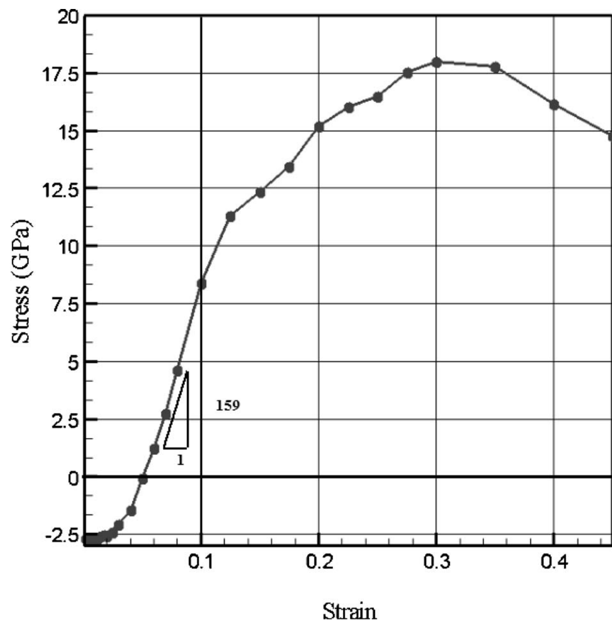

Fig. 4 Stress-strain curve for the near-surface ion bombarded material. A stress-free state is observed at a strain of about 0.05. Linear behavior is observed near the stress-free state, with an average linear modulus of 159 GPa.

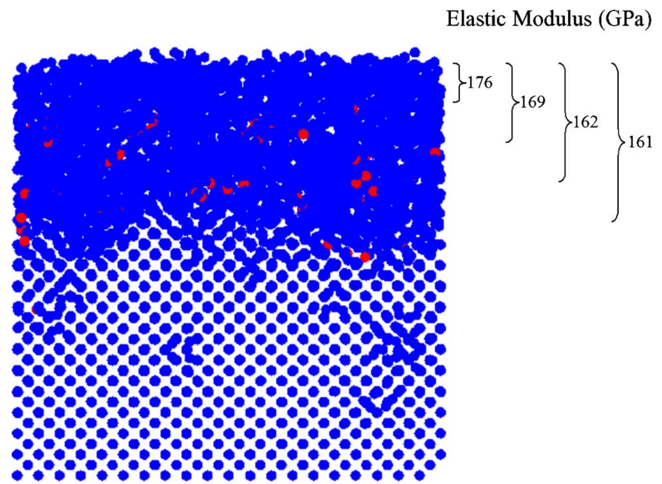

Fig. 5 Comparison of moduli (in GPa) computed over various depths from the surface. Nearest to the surface the apparent modulus is highest, while averaging over more of the "bulk" amorphous silicon leads to a lower modulus.

Cheung and Yip [17]. Interatomic forces acting on different cross sections of known area are calculated to find stress in the material. It is observed that the most of the damage-free, nearly crystalline material is stress free, while the damaged region in the material has a compressive stress as high as a few GPa [18]. It should be noted that while this damage-induced stress in the computational test specimen is large enough to induce phase transformations in silicon, and while the computational method does intrinsically account for this possibility, the constraints imposed by the boundary conditions and the short time scales preclude any such stress-induced transformation.

Extensional strain in the plane of the free surface, applied to the entire 5.43 nm cube silicon specimen, expands or contracts both the damaged and undamaged portions of the specimen. However, stresses are examined only over the predominantly damaged layer in order to obtain the stress-strain response in that region. After application of strain, the specimen is maintained at approximately 300 K for about a tenth of a picosecond, to allow the atom positions to relax. The specimen is then slow cooled to 77 K, followed by quenching to 4 K in order to freeze the structure and to minimize any kinetic contribution to stress before performing stress analysis. The constant strain is applied incrementally, and on multiple randomized cases.

The stress-strain curve is plotted in Fig. 4. The initially compressive stress in the material, due to the effect of the argon implantation and associated damage, gradually shifts to tensile stress as more strain is applied. A stress-free state is observed at a strain of about 0.05. Near the stress-free state, the ion-bombarded material follows a linear stress-strain relationship. The effective tensile modulus near the stress-free state, calculated from the slope of the stress-strain curve, is about 159+/−3 GPa. The Young's modulus calculated using nanoindentation coupled with a finite element model for a self-ion implanted amorphous silicon specimen has been reported in [19] to be 136+/−9 GPa without relaxation and 146+/−9 GPa after annealing for an hour at 500 °C. Though this agreement is encouraging, it is noted that the bombarding ion, fluence, beam energies, and implantation depths considered in [19] are very different from those used in the present work. The values calculated in this work correspond to a specimen bombarded with argon atoms, but with a comparatively low concentration of implanted argon.

Constant strain tests are performed up to a strain of 0.40. The stiffness gradually decreases as the strain exceeds 20%. Finally, the stress generated in the material decreases beyond a strain of 0.30 as the bonds weaken according to the Stillinger-Weber potential. Strains of this magnitude are unrealistically large; the results merely illustrate the essential features of the potential at large interatomic separations. Yield in the macroscopic sense is absent as no new deformation mechanisms become active in this highly disordered and confined region; the Stillinger-Weber atomistic model does inherently account for yield, fracture, and phase changes, but the computational test conditions—including time scales and boundary conditions—constrain against such mechanisms.

Finally, the presence of the free surface itself does have a small effect on the continuum elastic modulus as derived from the constant strain test. The undercoordination of surface atoms and the resulting implications for surface energetics via reconstructions, for example, can in turn affect the intrinsic stiffness of the free surface relative to the bulk. This effect can substantially alter the apparent moduli of nanoscale structural elements, as has been observed previously in studies of a variety of materials, including crystalline Stillinger-Weber silicon [20]. Depending on the surface energetics, and the relative tendency to reconstruct, materials may have either positive or negative surface stiffnesses associated with a particular crystallographic orientation; (001) crystalline Stillinger-Weber silicon surface have relatively large negative stiffness, so that nanoscale structures with perfect (001) free surfaces appear less stiff than corresponding bulk structures. In the present work on Stillinger-Weber silicon with an essentially amorphous near-surface layer due to ion bombardment, the free surface contributes a positive stiffness to the overall bulk response. Figure 5 shows that the computed stiffness is larger when the forces are computed over a thinner region nearest to the free surface, which implies that the surface is stiffer than the bulk. For the case illustrated in Fig. 5, the surface stiffening effect is at least 10%. This cannot be directly attributed to surface reconstructions, as the disordered surface does not admit regular reconstructions; nevertheless it is clearly related to the different coordination of the near surface atoms.

3.3 Mapping to a Continuum Surface. In order to fully connect the atomistic model for the ion-bombarded silicon to the continuum treatment needed to understand surface evolution, it is necessary from a practical perspective to map the discretized sur-

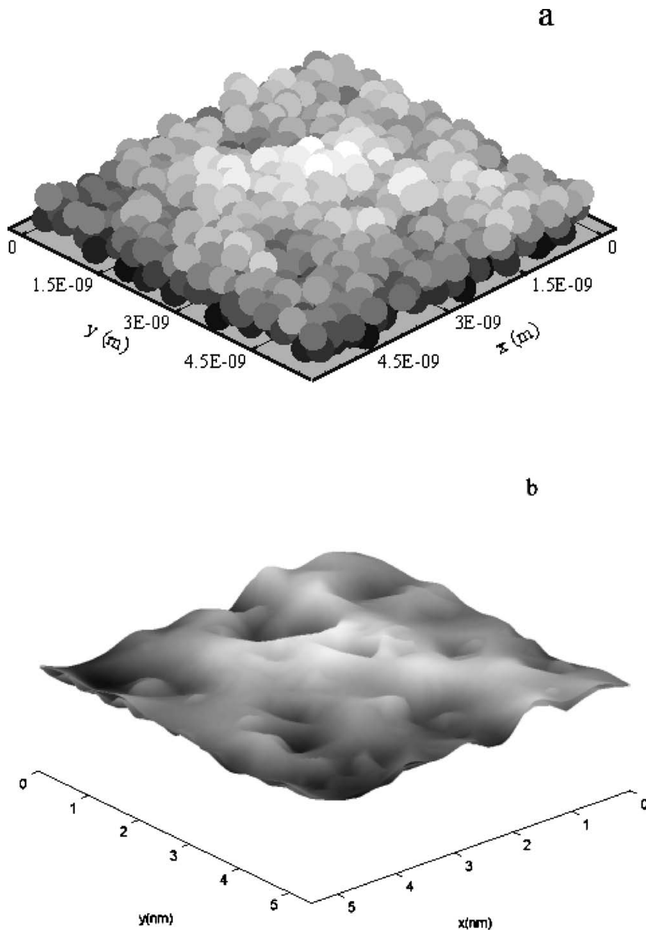

Fig. 6 (*a*) Near surface atomic positions of highly damaged silicon are shown after a fluence of 3.39×10^{14} ions/cm^2. The reconstructed continuum surface is shown in (*b*). The variation in surface height is approximately 0.3 nm, while on a crystalline [100] silicon surface it is computed to be approximately 0.03 nm by the method used here.

face onto a continuum surface given by an equation of the form $z=f(x,y)$, where z represents the surface height at coordinates (x,y). To avoid any arbitrariness, the surface is defined by calculating a set of points P above the specimen at which the force in the z-direction F_z experienced by a single-atom virtual silicon probe is zero. The set of points P is then said to belong to the surface S. For an ion-bombarded sample, the concentration of argon atoms at the surface is small. Therefore, F_z acting on a silicon atom due to the specimen's atoms near the surface is calculated. The method used here is similar to the use of a spherical probe in surface profilometers. Four hundred points that belong to the surface are calculated and interpolated to obtain equations representing the surface. Figure 6(*a*) shows the atomic positions near the surface of silicon bombarded to a fluence of 3.39×10^{14} ions/cm^2 and Fig. 6(*b*) shows the surface reconstructed by the method described above for the same specimen. The maximum variation in the continuum surface height for this disordered surface is approximately 0.3 nm, or ten times the variation seen for the equivalent perfect crystalline silicon surface based on this method.

4 Conclusions

Surface free energy density is calculated for the (001) surface of ion-bombarded silicon and compared to that of an unrelaxed crystalline silicon surface. In order to compare the results obtained from ion-bombarded specimen and the crystalline silicon an unreconstructed crystalline surface is studied, as there is no analog of reconstruction in an amorphous/damaged material. The extensional stress-strain relationship is computed for the near-surface ion damaged material by performing constant strain tests. The modulus close to a stress-free state is computed to be 159+/−3 GPa, which is in reasonable agreement with experimental observations, even though the material studied here is highly damaged and energetic. The presence of the free surface has a small stiffening effect on the overall modulus of the ion-bombarded material. Finally, a simple method is used to fit the atomistic surface of the ion-bombarded silicon with continuous functions, thereby making a complete connection to continuum surface models possible.

Acknowledgment

The authors gratefully acknowledge the support of NSF Grant No. DMI 02-23831.

References

[1] Bifano, T. G., Johnson, H. T., Bierden, P., and Mali, R., 2002, "Elimination of Stress Induced Curvature in Thin-Film Structures," J. Microelectromech. Syst., **11**, pp. 592–597.
[2] Bobek, T., Fackso, S., and Kurz, H., 2003, "Temporal Evolution of Dot Patterns During Ion Sputtering," Phys. Rev. B **68**, p. 085324.
[3] Hofer, C., Abermann, S., Teichert, C., Bobek, T., Kurz, H., Lyutovich, K., and Kasper, E., 2003, "Ion Bombardment Induced Morphology Modifications on Self-Organized Semiconductor Surfaces," Nucl. Instrum. Methods Phys. Res. B, **216**, pp.178–184.
[4] Ross, F. M., Tersoff, J., and Tromp, R. M., 1998, "Coarsening of Self-Assembled Ge Quantum Dots on Si (001)," Phys. Rev. Lett. **80**(5), pp. 984–987.
[5] Floro, J. A., Lucadamo, G. A., Chason, E., Freund, L. B., Sinclair, M., Twesten, R. D., and Hwang, R. Q., 1998, "SiGe Island Shape Transition Induced by Elastic Repulsion," Phys. Rev. Lett. **80**(21), pp. 4717–4720.
[6] Floro, J. A., Chason, E., Freund, L. B., Twesten, R. D., Hwang, R. Q., and Lucadamo, G. A., 1999, "Evolution of Coherent Islands in $Si_{1-x}Ge_x/Si(001)$," Phys. Rev. B **59**(3), pp. 1990–1998.
[7] Oura, K., Lifshits, V. G., Saranin, A. A., Zotov, A. V., and Katayama, M., 2003, *Surface Science An Introduction*, Springer-Verlag, Berlin.
[8] Moore, M. C., Kalyanasundaram, N., Freund, J. B., and Johnson, H. T., 2004, "Structural and Sputtering Effects of Medium Energy Ion Bombardment of Silicon," Nucl. Instrum. Methods Phys. Res. B, **225**, pp. 241–255.
[9] Gao, H., 1994, "Some General Properties of Stress-Drive Surface Evolution in a Heteroepitaxial Thin Film Structure," J. Mech. Phys. Solids **42**(5), pp. 741–772.
[10] Stillinger, F., and Weber, T., 1985, "Computer Simulation of Local Order in Condensed Phases of Silicon," Phys. Rev. B **31**, pp. 5262–5271.
[11] Molière, V. G., 1947, "Theorie der Streuung Schneller Geladener Teilchen I: Einzelstreuung am Abgeschirmten Coulomb-Field," Z. Naturforsch. A **2A**, pp. 133–145.
[12] Torrens, I. M., 1972, *Interatomic Potentials*, Academic Press, New York.
[13] Griffith, A. A., 1921, "The Phenomena of Rupture and Flow in Solids," Philos. Trans. R. Soc. London, Ser. A **221**, pp. 163–198.
[14] Stekelnikov, A., Furthmuller, J., and Bechstedt, F., 2002, "Absolute Surface Energies of Group-IV Semiconductors: Dependance on Orientation and Reconstruction," Phys. Rev. B **65**, p. 115318,
[15] Perez, R., and Gumbsch, P., 2000, "An Ab Initio Study of the Cleavage Anisotropy in Silicon," Acta Mater. **48**, pp. 4517–4530.
[16] Partyka, P., Zhong, Y., Nordlund, K., Averback, R. S., Robinson, I. M., and Ehrhart, P., 2001 "Grazing Incidence Diffuse X-Ray Scattering Investigation of the Properties of Irradiation-Induced Point Defects in Silicon," Phys. Rev. B **64**, p. 235207.
[17] Cheung, K. S., and Yip, S., 1991, "Atomic-Level Stress in an Inhomogeneous System," J. Appl. Phys. **70**, pp. 5688–5690.
[18] Kalyanasundaram, N., Moore, M. C., Freund, J. B., and Johnson, H. T., (unpublished).
[19] Follastaedt, D. M., Knapp, J. A., and Myers, S. M., 2004, "Mechanical Properties of Ion-Implanted Amorphous Silicon," J. Mater. Res. **19**(1), pp. 338–346.
[20] Miller, R. E., and Shenoy, Vijay B., 2000, "Size-Dependent Elastic Properties of Nanosized Structural Elements," Nanotechnology, **11**, pp. 139–147.